2022-12-15

Effect of X-Ray Illumination on Magnetic Domain Memory in [Co/Pd]/IrMn Multilayers

Colby Singint Walker
Brigham Young University

Effect of X-Ray Illumination on Magnetic Domain Memory in [Co/Pd]/IrMn Multilayers

Colby Singint Walker

A thesis submitted to the faculty of
Brigham Young University
in partial fulfillment of the requirements for the degree of

Master of Science

Karine Chesnel, Chair
Robert Davis
John Colton

Department of Physics and Astronomy

Brigham Young University

ABSTRACT

Effect of X-Ray Illumination on Magnetic Domain
Memory in [Co/Pd]/IrMn Multilayers

Colby Singint Walker
Department of Physics and Astronomy, BYU
Master of Science

This thesis focuses on investigating the possible x-ray illumination effects on the magnetic domain memory (MDM) in magnetic [Co/Pd]IrMn multilayers. In this material, MDM is induced via exchange couplings between the ferromagnetic Co/Pd layer and the antiferromagnetic IrMn layer. To carry out this investigation, we have used magneto-transport and x-ray resonant magnetic scattering. The use of magneto-transport in-situ at synchrotron x-ray scattering facility has allowed us to follow the gradual effect of x-ray illumination on the amount of exchange bias, initially present after field cooling the material. With our in-situ measurements we have been able to see that x-ray illumination does have an effect on the strength of exchange couplings in our material. To support this observation, we have also carried out complementary measurements at home in a cryomagnet, at various temperatures between 300K and 25K, and in a variety of configurations.

Keywords: exchange bias, magnetic domain memory, magneto-transport, exchange couplings, antiferromagnet, ferromagnet

ACKNOWLEDGMENTS

I want thank everyone who helped me to get to this point, as well as my Mother and Father for supporting me in everything I do. I want to thank my graduate advisor Dr. Karine Chesnel, for mentoring me in carrying out research through the years, this includes taking the time to instruct me in the use of our experimental instruments, paying for travel to many different conferences, and the countless hours spent reading and editing this thesis. I would also like to thank the other members of my Committee, Dr. John Colton, and Dr. Robert Davis, for being willing to spend time reading and editing my thesis. Lastly I want to thank the BYU physics department for funding my research for the past few years.

Contents

List of Figures

Chapter 1

Introduction

1.1 Exchange bias in magnetic multilayers

The material we are studying is a $[[\mathrm{Co}(4\text{Å})/\mathrm{Pd}(7\text{Å})]_{12}/\mathrm{IrMn}(24\text{Å})]_4$ multilayer for which the structure is illustrated in Fig.1.1 . The [Co/Pd] layer is ferromagnetic. Ferromagnetism (FM) is when the atomic spins (here carried by the atoms of Co) align parallel to each other. The IrMn alloy forms the antiferromagnetic part of the material. Antiferromagnetism (AFM) is when the atomic spins (here carried by the atoms of Mn) align anti-parallel. Our material exhibits what is called a perpendicular magnetic anisotropy (PMA) which means that the net magnetization points out of plane. The magnetic anisotropy is "the energy that it takes to rotate the magnetization direction from easy into the hard direction." [1]. When a FM/AFM interface is formed, it exhibits material exhibits exchange bias. The bias is the result of uncompensated moments at the interface of the AFM and FM layers. In order to create exchange bias the material must be field cooled (FC) below its blocking temperature, T_B which is ~300K. The spins pinned by FC remains locked when below the T_B and create a net (non-zero) field at the interface (the bias). This causes the hysteresis loop to shift horizontally to the direction opposite to the field previous applied during the FC. We measured

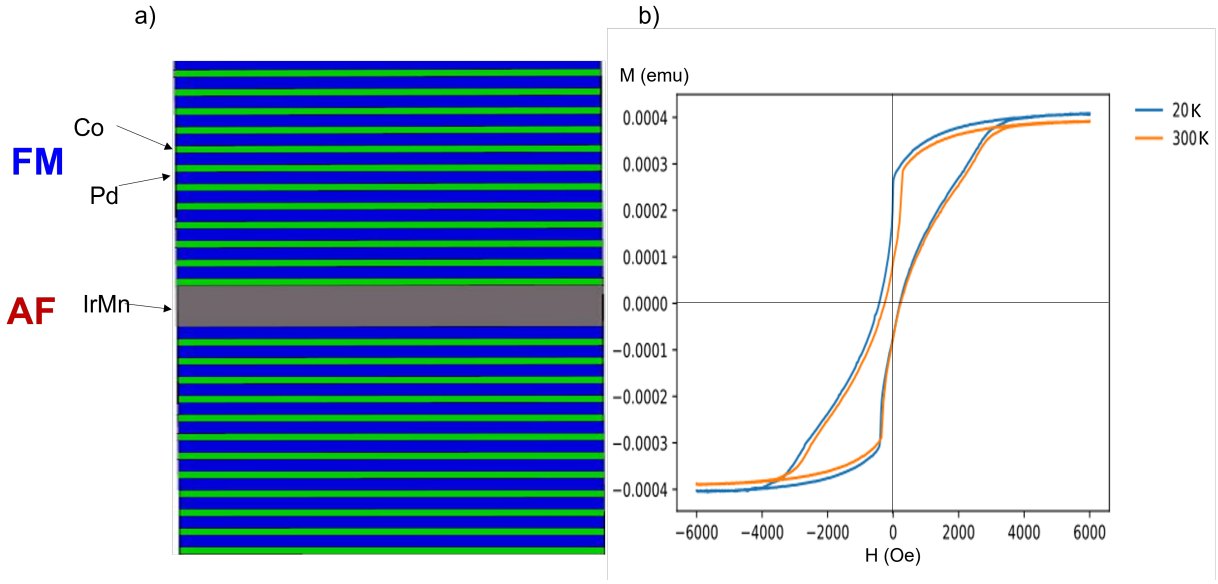

Figure 1.1 a) Cross section through [Co/Pd]/IrMn multilayer. The Co/Pd multilayer is ferromagnetic. The IrMn alloy is antiferromagnetic. b) Magnetization loops measured via VSM at 300 K and at 20 K after field cooling under a field of 4000 Oe. The blue loop measured at 20 K exhibits an exchange bias of about 200 Oe.

a bias field of around -200 Oe at 20K after field cooling under a saturating field of 4000 Oe. This bias is the physical manifestation of exchange coupling interactions between the FM [Co/Pd] and the AFM IrMn layers. These exchange couplings allow the pattern in the FM layer to imprint the AFM layer when the sample is field cooled, which leads to creates magnetic domain memory.

1.2 Magnetic Anisotropy and Magnetic Domains

When a magnetic field is applied to a ferromagnetic material (either in plane or out of plane), the atomic magnetic moments eventually all align with the applied field (saturation point). Below saturation, or in the absence of field, the material starts to form multiple magnetic domains, each exhibiting a different direction for the magnetization. For materials with PMA, the magnetization is mostly out-of plane, either up or down. This leads to the formation of domain patterns with

Figure 1.2 Illustration of a magnetic domain pattern with magnetization directed up and down out-of-plane.

magnetization pointing alternately up and down from one domain to the next one, for example alternating spins of up and down. Fig. 1.2 illustrates an example of what a magnetic domain pattern looks like. In a PMA thin film, these magnetic domains naturally form in order to reduce the total magnetic energy. It should also be noted that there are two different types of anisotropies: shape anisotropy and magneto-crystalline anisotropy. The former is due to the shape of the material and the latter is due to the spin orbit interaction. The direction for the easy axis is determined by the competition between both of these. The PMA in our material is mostly caused by the shape anisotropy.

1.3 Magnetic Domain Memory

Magnetic domain memory (MDM) is a property of a magnetic material to retain the domain patterns under field cycling. MDM is normally absent in single AFM layer. Here, MDM is induced via exchange couplings between the FM and AFM layers. When field cooling, the FM layer imprints a pattern on the AFM layer. Upon field cycling the same exact magnetic domain pattern reforms, driven by the magnetic domain template imprinted in the AFM layer.

The way we probe MDM is by using coherent x-ray magnetic scattering (c-XRMS). Speckle

patterns are collected at various field values throughout the magnetization cycle, in successive cycles. The collected speckle patterns are then used to calculate cross-correlation coefficients which are then assembled into a correlation map. A speckle pattern essentially represents the magnitude of the Fourier transform of the particular magnetic domain pattern (the phase is lost). If the resulting speckle pattern has the shape of a ring, then the magnetic domain pattern itself does not have a preferred direction. See Fig. 1.3 illustrates an example of a speckle pattern. In the speckle pattern, the speckle spots are not directed in a particular direction.

1.4 Research problem: study possible illumination effects

While carrying XRMS measurements of MDM, we noticed that x-ray illumination from synchrotron radiation sources may result in the loss of exchange coupling between the FM and AFM layers. The purpose of my research project is to study the possible effects of X-ray illumination on exchange bias (EB) and consequently, on MDM. Applications of MDM are in the area of magnetic storage. It is important to know if the photon illumination can possible affect the strength of MDM The ability to control MDM by tuning the amount of light we shine onto the material can lead to numerous applications including in magnetic recording. We anticipate that the results from this study will likely lead to publications. In an article [2] the following was stated "can the number of pinned uncompensated moments be manipulated by external means such as stress, light, and electric field". We are seeking to answer part of this question and see if it is related to the observed loss of MDM in our [Co/Pd]/IrMn thin films.

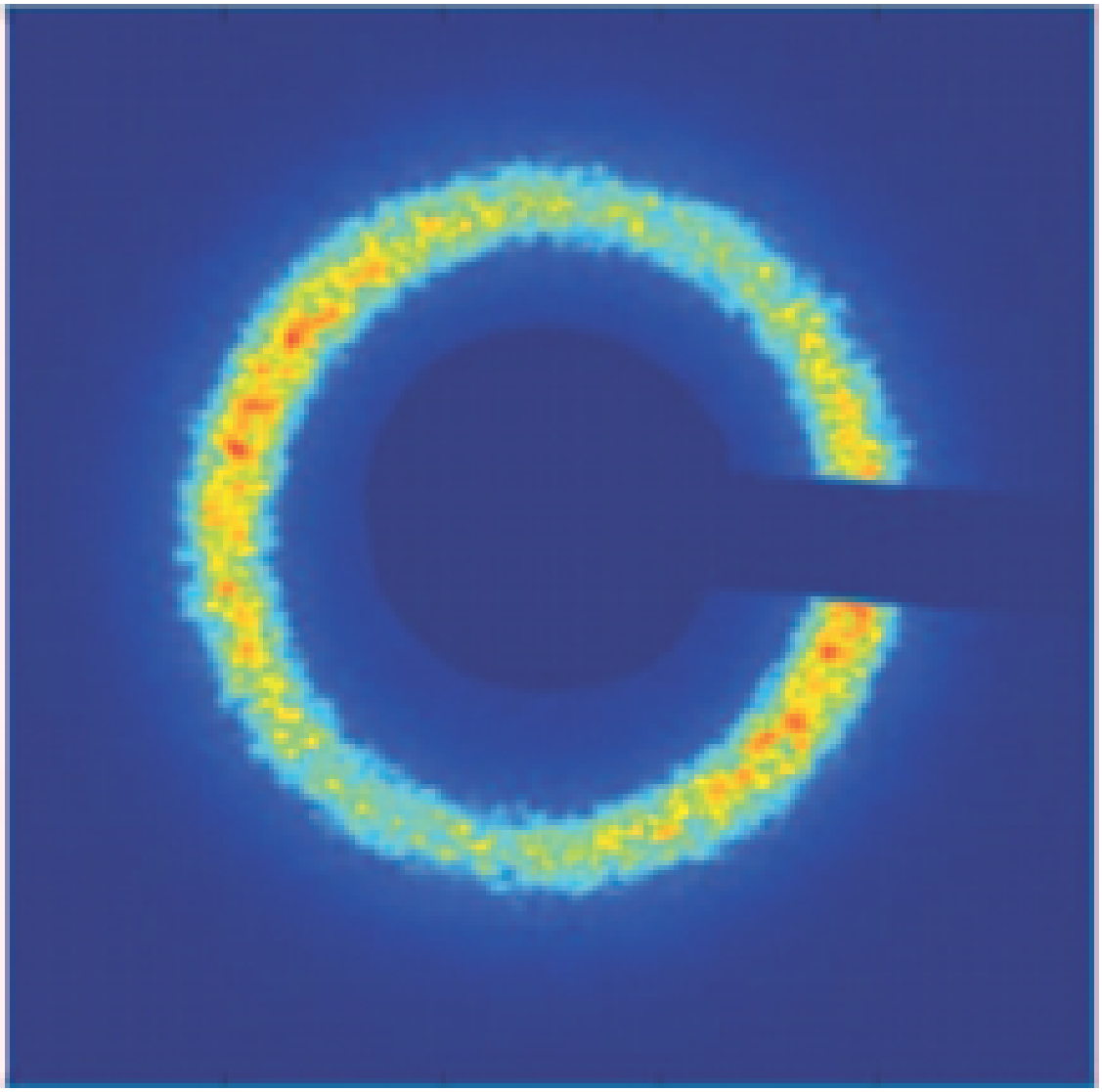

Figure 1.3 Example of speckle pattern collected on [Co/Pd]/IrMn multilayers with coherent x-rays, whose energy is tuned to Fe-L_3 edge at around 708 eV.

Chapter 2

Experimental Techniques

In this chapter we will discuss the experimental techniques used in my research project, including magnetometry, magneto-transport and x-ray magnetic scattering.

2.1 Vibrating Sample Magnetometry (VSM)

The purpose of magnetometry is to measure the magnetic response of materials when subject to a magnetic field. Vibrating Sample Magnetometry (VSM) is one way to access this information. VSM is based on the Faraday effect, where the change of the magnetic flux through a loop induces an electromagnetic voltage. To implement this, the sample is vibrated through a pickup coil. The vibration of the magnetic material induces a change in magnetic flux through the pickup coil, which itself induces a voltage (or "electromagnetic force") in the pickup coil [3]. The measured induced voltage is assumed to be proportional to the magnetization of the sample. The instrument is calibrated so that the units of the measured magnetization M is "emu" (electro-magnetic unit).

Fig. 2.1 shows a diagram of the VSM instrument. A motor at the top of the instrument drives the vibration of the sample. The driving frequency of the vibration is around 60 Hz. The vibration occurs while a magnetic field is applied to the sample. The applied magnetic field H is produced by

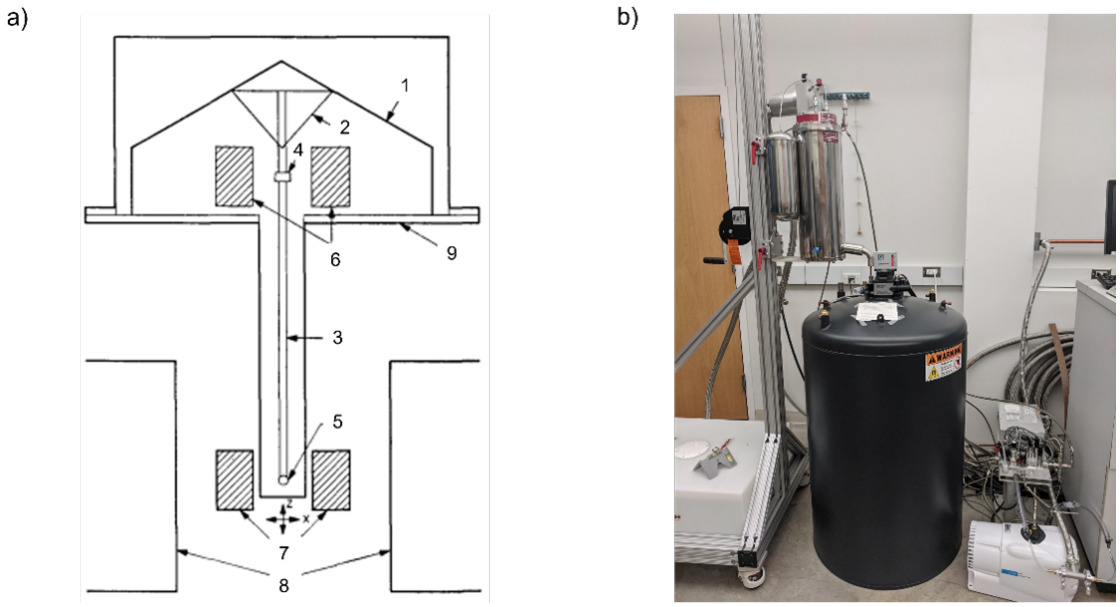

Figure 2.1 . a) Diagram of the VSM, including (1) motor or transducer for driving vibrations, (2) support, (3) sample holder, (5) sample, (7) sample coils, (8) superconducting magnet. b) Picture of our VSM instrument at BYU.

a superconducting magnet located at the center of the instrument. The voltage induced in the pickup coil is proportional to the magnetization M of the material at a given field H. The magnetic field H can be set to any value from 0 to 9 T. In order to operate, the superconducting magnet needs to bathe in liquid helium. A lack or low liquid helium supply could lead to damage to the superconducting magnet. A proper measurement requires that the sample is centered at the center of the pickup coil. Additionally, the instrument possesses a cryostat. The temperature of the sample can be varied from a maximum value of 400 K down to around 1 K with the assistance of liquid helium. Being able to heat up the sample to 400 K may be useful for getting rid of any remanent magnetization. The instrument operates in vacuum.

The VSM can be used to measure magnetic hysteresis in ferromagnetic material. Fig. 2.2 shows an example of hysteresis loop measured via VSM on our [Co/Pd]/IrMn films, where the magnetization M is plotted against the applied field H. It reflects the magnetic response of the

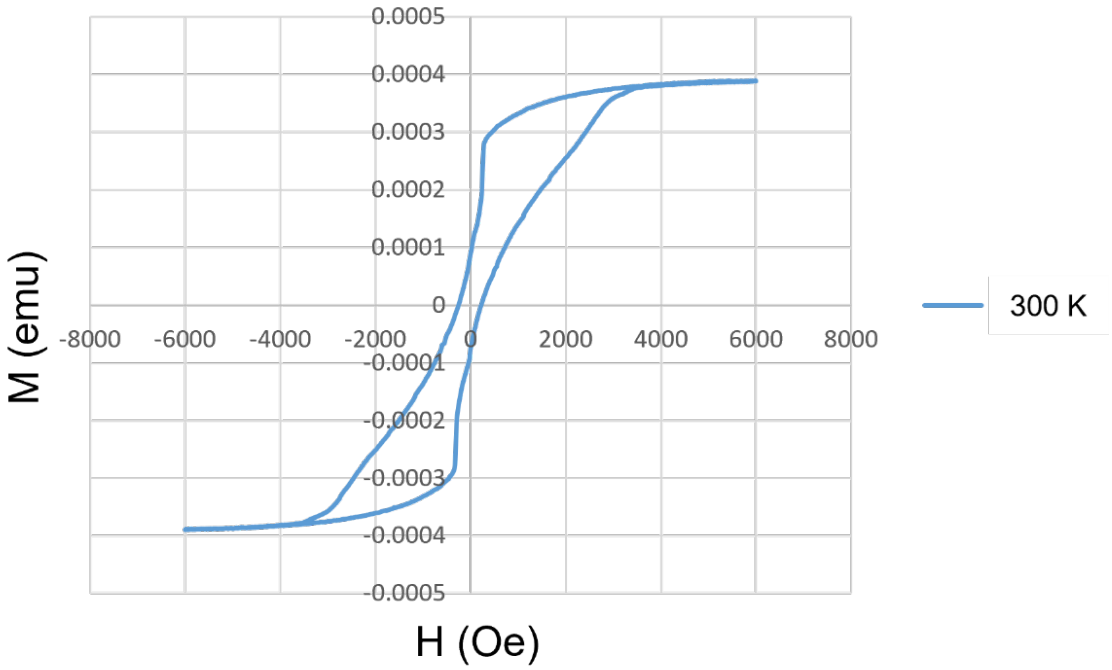

Figure 2.2 Magnetization loop measured via VSM on our [Co/Pd]/IrMn film at 300 K

material to an externally applied field. The VSM can also be used to measure the magnetization as a function of temperature M(T). This is useful to study materials that exhibit a magnetic transition, and for finding the temperature at which magnetic transitions happen (for example, blocking temperature).

The magnetization M is the averaged magnetic moment per volume. For FM material presenting nanoscale magnetic domains where the magnetization is pointing in different directions, the VSM just outputs the macroscopic averaged magnetization, averaged over all the microscopic domains. The field value at which M starts plateauing is called the saturation field H_s. For the material we are studying $H_s = 3200$ Oe at 300K. Below saturation (when $H < H_s$) the magnetization in the various domains may point in different directions. Once the material has reached saturation ($H = H_s$), the magnetization points uniformly in the same direction throughout the sample, and M reaches its maximum value M_s (magnetization at saturation).The nucleation field (H_n) is the point on the

descending branch of a magnetization loop where M starts to decrease again. The coercive field (H_c) is the field that need to be applied in order to bring M back to zero. The magnetization loop is symmetrical, meaning the descending and ascending branches reflects each other. The coercivity is important to quantify, because this is how we will later estimate the amount of bias, in the presence of exchange bias. For our [Co/Pd] IrMn multilayers, H_c ~200 Oe at around 20K.

2.2 Magneto-Transport

Magneto-transport is essentially the measurement of transport properties in the presence of magnetic field and/or for magnetic materials. It includes two categories of signal: 1) magneto-resistance (MR), and 2) Hall effect (HE) signals, which we describe below.

The Hall effect signal provides another way to measure hysteresis magnetization loops in magnetic materials [4]. When measuring HE in magnetic materials, one needs to consider two components: 1) the regular "ordinary" Hall effect, induced by the external field; and 2) the "extraordinary" Hall effect (EHE), included by the internal fields. For non-magnetic, but conductive materials, the Hall voltage measured across the sample is simply the ordinary Hall effect signal proportional to the applied field H. For magnetic material, the additional EHE voltage is assumed to be proportional to the magnetization M of the sample. In our ferromagnetic materials, the EHE component largely dominates the ordinary Hall effect (no need to subtract it to visualize the EHE signal).

In order to carry a EHE measurement on our ferromagnetic films with PMA, we need to first apply a field perpendicular to the surface of the sample (out-of-plane) as illustrated in Fig. 2.3. Next, we need to apply a current in-plane and measure the voltage in the transverse direction in the plane of the film. The origin of this effect can be described by the Lorentz force ($F = q\mathbf{E} + q\mathbf{v} \times \mathbf{B}$), that governs how charged particles (electrons, in this case) move under the influence of a magnetic

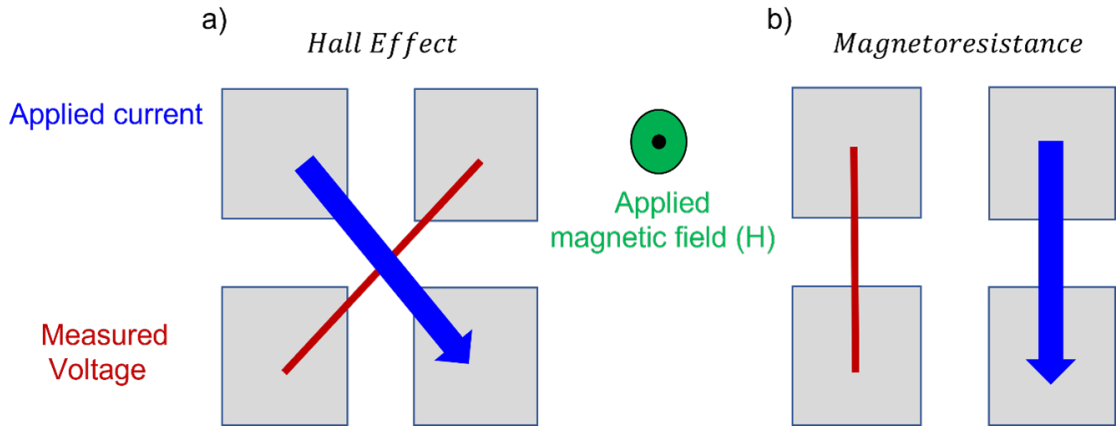

Figure 2.3 Diagrams showing how current is applied and voltage is measured for a) Hall Effect (cross configuration) and b) Magnetoresistance measurements (parallel configuration)

field. When the electrons from the applied current move and enter the influence of the applied field, they are deflected sideways, and this creates a Hall voltage. q**v** x **B** is a mathematical expression for a sideways deflection of a charged particle. In order to get rid of any asymmetries in the data due to the placement of the contacts we need to permute the arrangement of the contacts for the current and voltage, respectively.

For HE measurements (illustrated in Fig. 2.3), there are two different arrangements, obtained by switching the directions of the current and voltage, respectively. Once both arrangements are measured, we average them in order to eliminate asymmetries in the placement of the contacts. It can be very difficult to place the contacts perfectly symmetrically enough such that there are no asymmetries in the data. The averaging technique generally eliminates asymmetries. Fig. 2.4 is what the surface of sample looked like with the Pt pads deposited on it using Focused Ion Beam (FIB) for making the contacts.

For the MR measurement, the field is still applied OOP, but the applied current and measured voltage are now parallel, as shown in diagram Fig 2.3b In the Van-der-Pauw averaging method [5], data is collected in four different permutations of the contacts. The data collected in the four

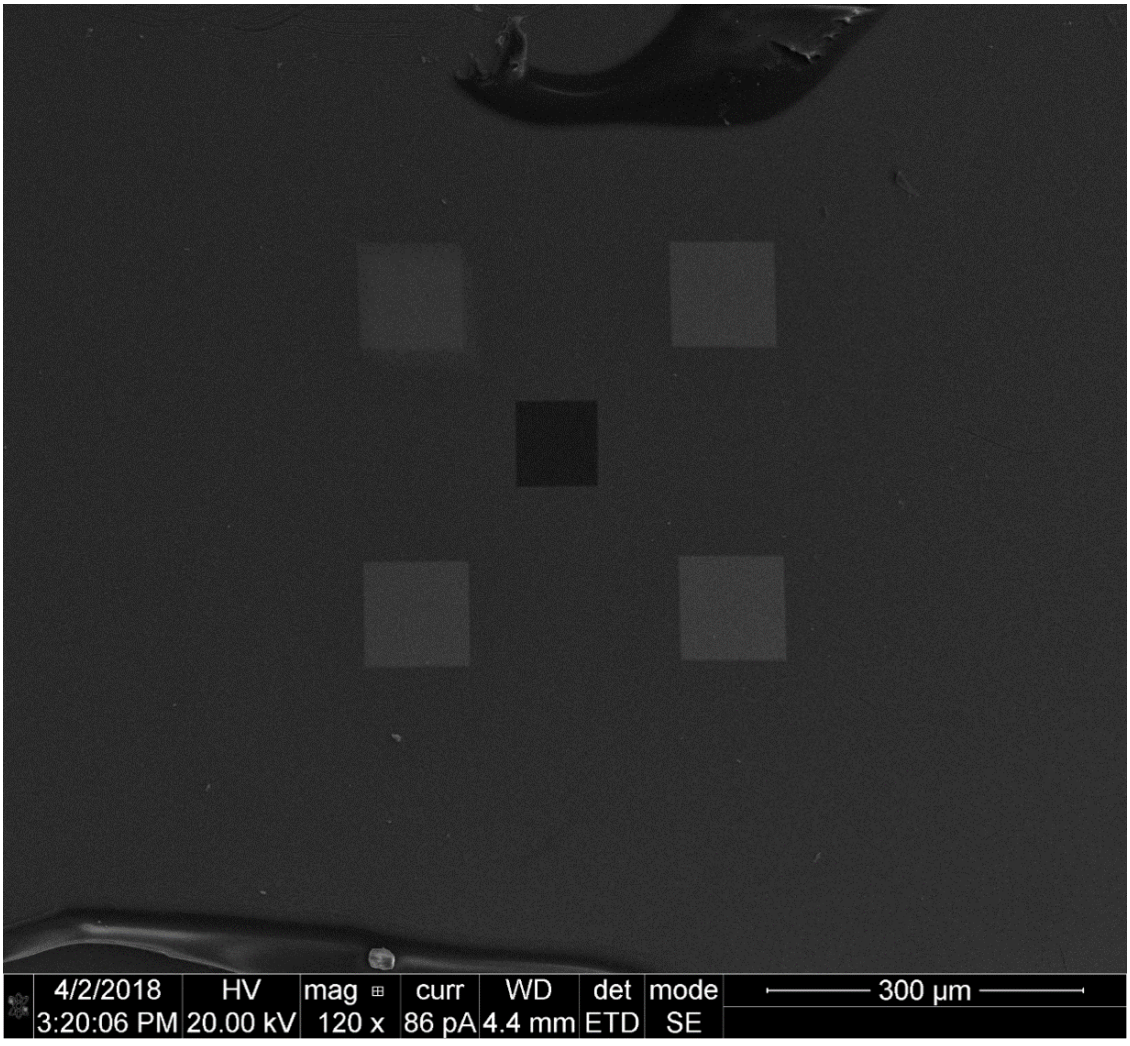

Figure 2.4 SEM image showing a top view of the [Co/Pd]/IrMn film, with the 100 μm window at the center, surrounded by four Pt pads at a distance of about 300 μm of each other.

different configurations is then averaged to eliminate any asymmetries coming from the contact positioning.

2.3 X-ray magnetic scattering

In addition to magnetometry and magneto-transport, we collected x-ray magnetic circular dichroism (XMCD) and x-ray resonant magnetic scattering (XRMS) data at synchrotron x-ray facilities. In the shape of a ring, a synchrotron facility sends electrons around the ring near the speed of light. Complex sets of magnets, called insertion devices, are used to control the trajectory of the electron beam, so it follows the circular path. As it goes around the ring, the act of bending the electron beam (bremsstrahlung effect) produces a synchrotron light, that covers a wide range of x-rays energies from soft x-rays to hard x-rays. The produced synchrotron x-ray beam then goes through advanced optics which are placed and designed to get the x-rays to where they need to go. One type of insertion device are undulators. An undulator is an array of magnets arranged in a periodic way that causes the beam to bend radially which causes another release of photons. As these photons travel down the undulator their phases match, thus producing a more coherent beam of photons. Additionally, the beamline may include optical components such as monochromators, allowing to tune the energy, as well as polarization plates, allowing to polarize the x-ray light.

Both XMCD and XRMS are element selective techniques. Tuning the energy to the absorption edge of the particular magnetic element provides the necessary magneto-optical contrast [3]. This allows to select different elements in the different layers of the material. In the case of transition metals, such as Co or Fe, one typically exploits the electronic transition between the 2p and 3d electronic bands ($L_{2,3}$ edges) [6]. For rare earth elements, the $L_{2,3}$ edges land in the hard x-ray region, but in the soft x-ray region are also the 3d to 4f transition available (M edges), although the 2p to 3d transition tends to provide more magnetic contrast. For our [Co/Pd]/ IrMn materials we

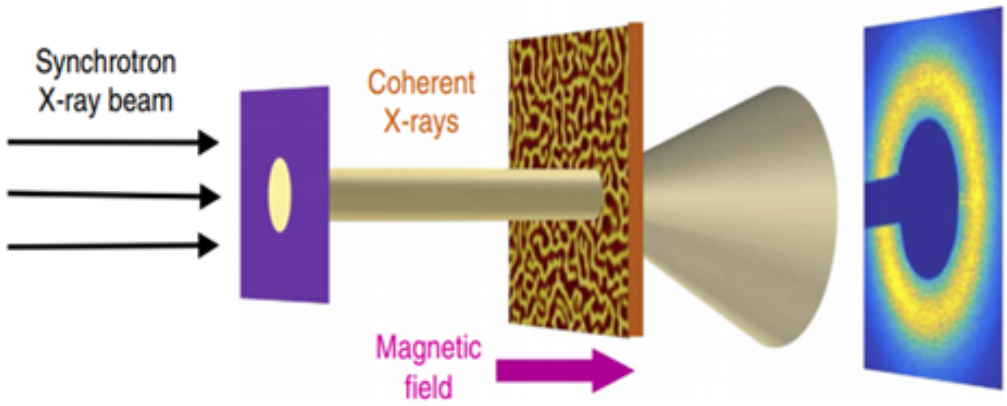

Figure 2.5 Layout for the x-ray resonant magnetic scattering (XRMS) experiment, with resulting speckle pattern. Extracted from [7]

use the Fe- $L_{2,3}$ at around 700 eV, which is in the soft-ray range (below 1 keV). At these energies, the wavelength of the light is a few nanometers, which is well suited to study nanoscale magnetic domains. When using soft x-rays, XMCD and XRMS measurements must be carried in vacuum to prevent the light to be absorbed by air. In order to carry out these measurements, the sample must therefore be in a vacuum chamber. From the undulator the coherent x-rays travel down the beamline where it gets to the beamline end station. Once it makes it to the sample, the coherent soft x-rays interact with the electron spins in the matter and will be scattered. The scattered light results in a speckle pattern which is collected on a CCD detector, as illustrated by Fig. 2.5.

2.4 Speckle correlation

The speckle patterns collected on the CCD camera are unique fingerprints of the magnetic domains patterns. For our MDM investigation, cross-correlating these patterns then allows one to detect any change in the magnetic domain patterns as the external magnetic field is being cycled. The process of cross-correlating involves recording two speckle patterns at two distinct magnetic field

values. The similarity between two speckle patterns is quantified by multiplying the intensity of the speckle pattern pixel by pixle after shifting one pattern with respect to the other one [7]. This process generates correlation patterns, which usually exhibit a correlation peak at their center. The correlation peak is integrated, which results in a number ρ that is normalized with respect to the square root of the product of the autocorrelations. The end result of this computation is a number, ρ between 0 and 1 that expresses how similar two distinct speckle patterns are. When the two patterns are exactly the same, $\rho = 1$, and when they are completely different, $\rho = 0$. A high degree (ρ close to 1) of MDM (i.e. a high correlation coefficient) means that the magnetic domains pattern in real space is unchanged. On the other hand, a low degree (ρ close to 0) of MDM means that the magnetic domain patterns are significantly different. Fig. 2.6 shows an example of correlation map measured on [Co/Pd]/IrMn at 20K after zero field cooling. The horizontal and vertical axes represent the two different field values, H_1 and H_2, at which the two correlated speckle patterns were collected.

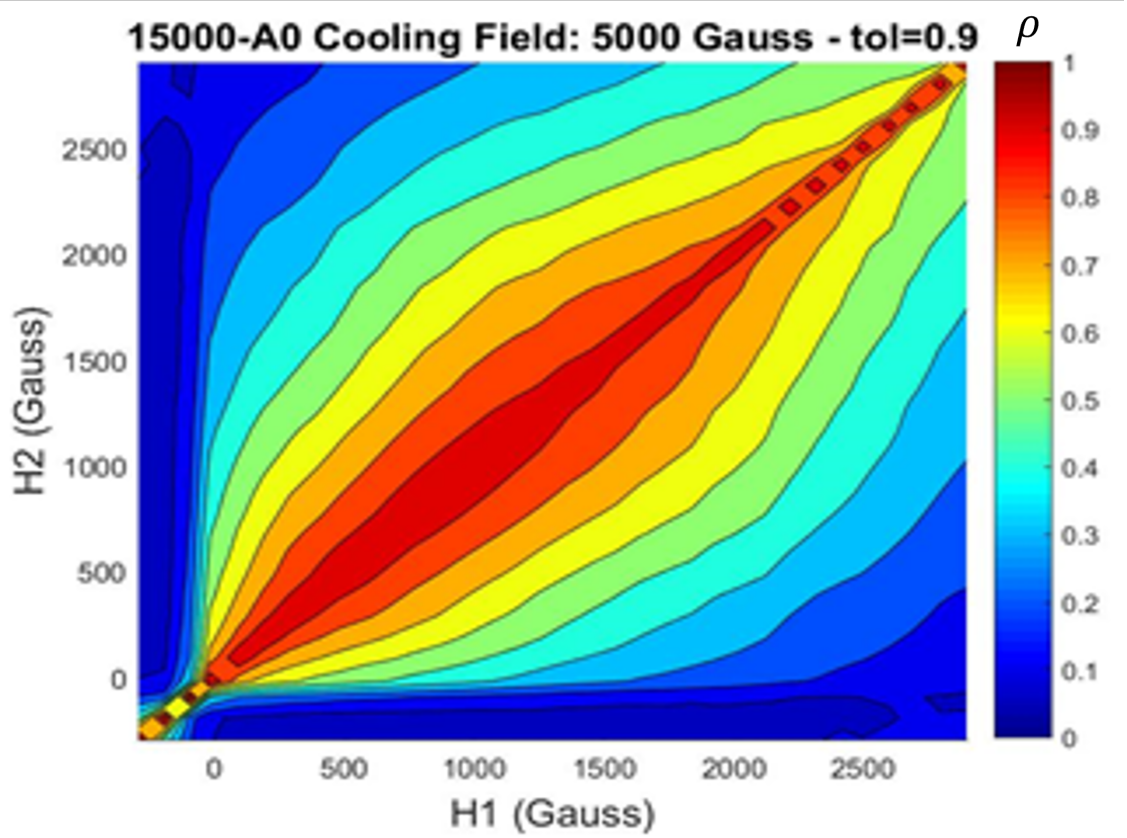

Figure 2.6 Correlation map, the horizontal and vertical axes represent two different field values H_1 and H_2 at which the two correlated speckle patterns have been collected. The quantity being plotted is the correlation coefficient, with blue being low ($\rho < 20$ %) and red being high ($\rho = 100$ %).

Chapter 3

Experiment

3.1 MDM measurements

In the previous chapter, we discussed how correlation maps are created. These are used to quantify how much memory the material has. For a regular ferromagnetic film, MDM is expected to be low, near zero, because when the field is cycled through an entire major loop and set back to the same initial value, the new magnetic domain pattern shows a different random arrangement of the domains compared to the initial one, even though the average magnetization is the same. In this case, when scattering patterns are cross-correlated over different cycles, the amount of MDM would be nearly zero. Non-zero MDM is a remarkable effect that is only observed in specific materials. Previous experiments have shown a strong amount of MDM under various conditions, including zero field cooling and cooling under a moderate field, as illustrated in Fig. 3.1 MDM appears when the temperature of the material is brought below the blocking temperature T_B. When $T < T_B$ the spins in the ferromagnetic and antiferromagnetic layers start to interact via exchange couplings.

This interaction will cause the domain pattern in the ferromagnetic layer to imprint onto the antiferromagnetic layer via the uncompensated at the interface. The imprinted AFM domain pattern

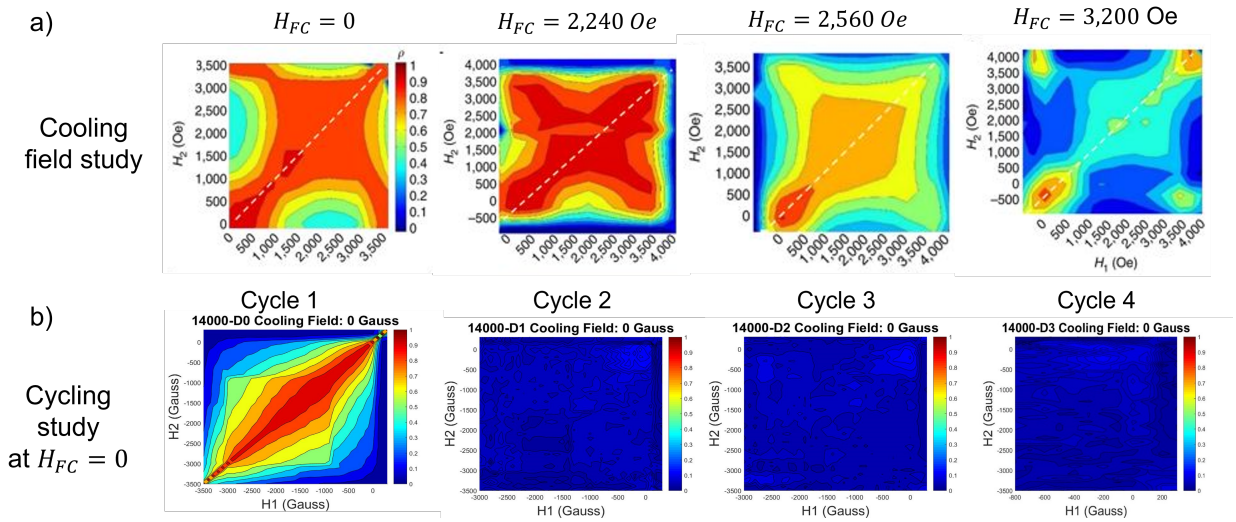

Figure 3.1 Correlation maps showing various amounts of MDM in [Co/Pd]/IrMn. (a) The first row is shows correlation maps collected at 20 K under different field cooling conditions where the magnitude of the cooling field varies from 0 up to 3200 Oe. (b) The second row shows correlation maps all collected after successive field cyclings at 20 K after the same zero field cooling process.

will then serve as a template for the domains in the F layer to nucleate and reform the same way over cycling and thus lead to a high degree of MDM. The materials we are studying here have been optimized to enhance the MDM effect by exploiting exchange bias between the FM and AF layers. The Chesnel group has observed up to 100% of MDM in [Co/Pd]/IrMn in various field cooling conditions [7–13].

3.2 Observed MDM loss

Previous measurements have demonstrated high MDM when field cooling [Co/Pd]/IrMn under zero or moderate field [7]. The first row of correlation maps in Fig. 3.1 shows correlation maps that have been measured in different cooling conditions, where the magnitude of the cooling field is varied from 0 to near saturating field 3200 Oe. Each of these maps has been averaged over several cycles. These maps show a relatively high amount of MDM in various field cooling,but the highest amount

of MDM is observed in Zero Field cooling (ZFC) where ρ reaches up to 100% extending on a wide range of field values throughout. The amount of MDM diminishes when the cooling field values approaches the saturation field, but MDM remains somewhat high (up to 50%) near nucleation and saturation (corners of the map) [7].

The correlation maps on the second row of Fig. 3.1, report correlations on successive cycles measured at 20 K after zero field cooling. It shows a complete loss of MDM after the first cycle. It is worth mentioning that the correlation maps on the first and second rows were collected at two different synchrotron facilities (ALS and APS respectively) under different illumination conditions. For the ALS data, a beam chopper was used, limiting the illumination time to brief periods, separated by no-illumination periods. For the APS data, no beam chopper was available so the sample was continuously illuminated by the x-ray beam for long period of time. After having done many different studies of MDM on our [Co/Pd] IrMn multilayers, we observed this unexplained loss of MDM after cycling the field. The loss of MDM was first noticed during experiments at the APS. The loss of MDM suggests disruption in the exchange couplings occurring between the Co/Pd ferromagnetic and the IrMn antiferromagnetic layer. However, it was found more recently that when under different illumination conditions, the material exhibited an unexpected loss of MDM, where the correlation coefficient was nearly zero throughout the entire magnetization loop, even in ZFC state. This loss of MDM may be due to the amount of x-ray illumination which may alter the strength of the exchange couplings between the ferromagnetic Co/Pd and antiferromagnetic IrMn layers. Consequently, a question is if this disruption in exchange couplings may be caused by increased x-ray illumination duration.

3.3 Probing exchange bias via in-situ magneto-transport

In order to investigate the MDM loss, our approach is to examine the exchange bias and its possible alteration under x-ray illumination. There are a few different ways to measure exchange bias in the FM/AFM layer. These various ways include magnetometry (VSM), x-ray magnetic circular dichroism (XMCD), and magneto-transport (MT). For investigating the effect of illumination on MDM and exchange bias, VSM would not be a good option, as it necessitates mechanically vibrating the samples and the VSM equipment is too bulky to fit in a x-ray scattering chamber. In order to investigate the effects of x-ray illumination we need to keep the synchrotron beam aligned with a micrometric transmission window on the sample. Vibrating the sample would lead to losing the alignment. XMCD would also not be a good choice either for measuring the effect of x-ray illumination because the XMCD signal contrast is dependent on the amount of illumination. As the beam intensity is decreased the signal becomes noisier. The last choice is magneto-transport (MT). For our specific study, MT fits our needs perfectly as it is independent of both vibrations and amount of illumination. Fig. 3.2 shows the MT setup we used to collect data at the Advanced Photon Source, at Argonne National Laboratory. The EHE signal measured around the transmission window on $[\mathrm{Co}/\mathrm{Pd}]/\mathrm{IrMn}$ films at the synchrotron facility shown in Fig. 3.3 an unusual shape, looking like a distorted magnetization loop. We see how the signal to noise is improved by increasing the amplitude of the applied current.

3.4 Complementary ex-situ magneto-transport measurements

In order to understand the distorted shape of the magnetization loop measured around the transmission window in Fig. 3.3, we carried separate measurements at BYU outside the synchrotron beamline. These measurements were carried at different locations of the samples for comparison purposes: on the inner contacts around the transmission window and on some outer contacts far

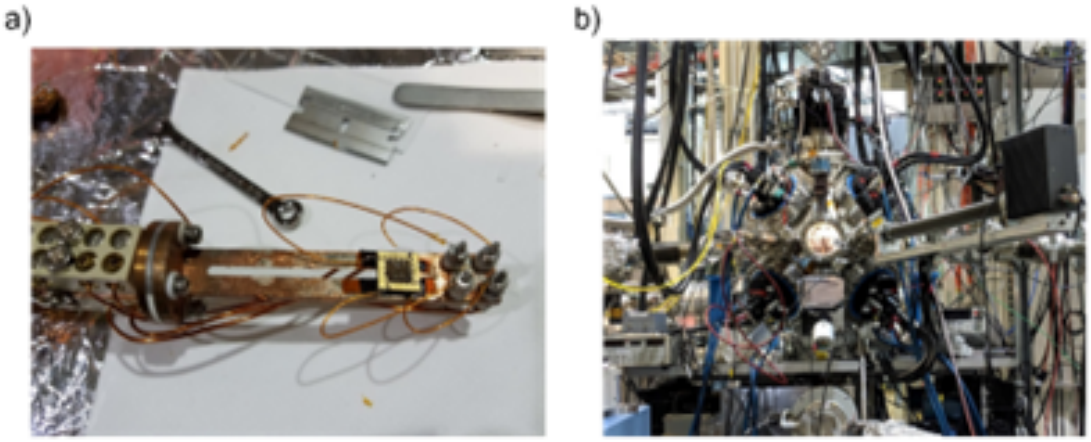

Figure 3.2 Illustration of the magneto-transport setup we used at the Advance Photon Source, at the Argonne National Laboratory (APS). a) Sample holder with electrical connections to be inserted into the vacuum scattering chamber, b) X-ray magnetic scattering chamber where the magneto-transport measurements were carried out at the APS.

away from the window as schematically illustrated in Fig. 3.4b.

The initial inner contacts were placed around the central transmission window such that they are 300 μm microns from each other, as seen in the SEM image Fig.3.4a. A third set of contacts were placed at macroscopic distances of each other. For this macroscopic set, for the outer contacts, the wirebonds have been placed on the edge of the sample which are about 5 mm apart for all these contacts sets. Two different measurements were carried out, one in a cross configuration for the EHE signal and one on the parallel configuration for magneto-resistance MR. By comparing the measurements on the inner and outer contacts, we were able to identify the source of the asymmetry in the data taken from the APS. We found that the source of the asymmetry was from the closeness between the electrical contacts located around the transmission window.

In the next Results chapter, we describe our quantitative findings on how this contact closeness causes data distortion.

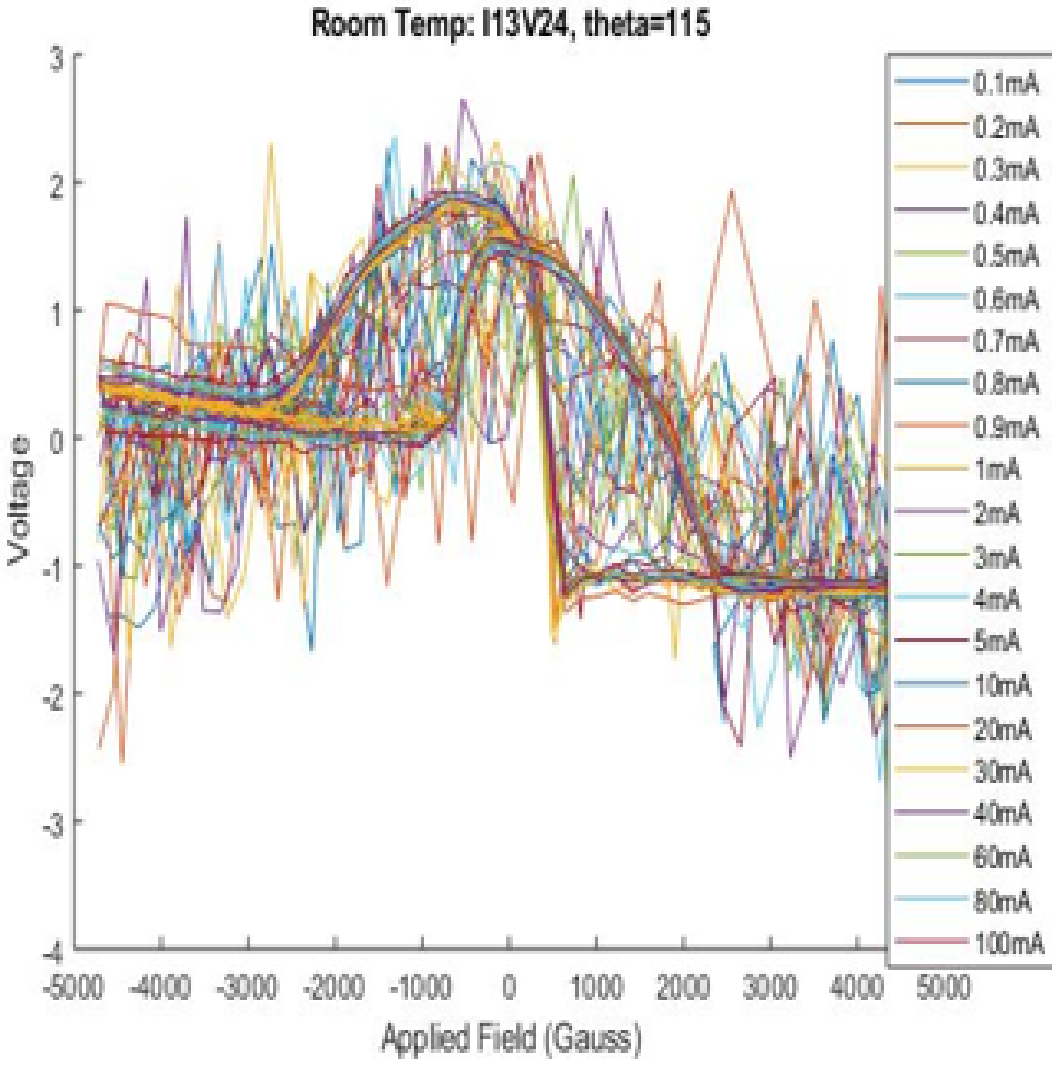

Figure 3.3 Synchrotron in-situ EHE loops measured at 300 K with different applied current values and in the absence of x-ray illumination.

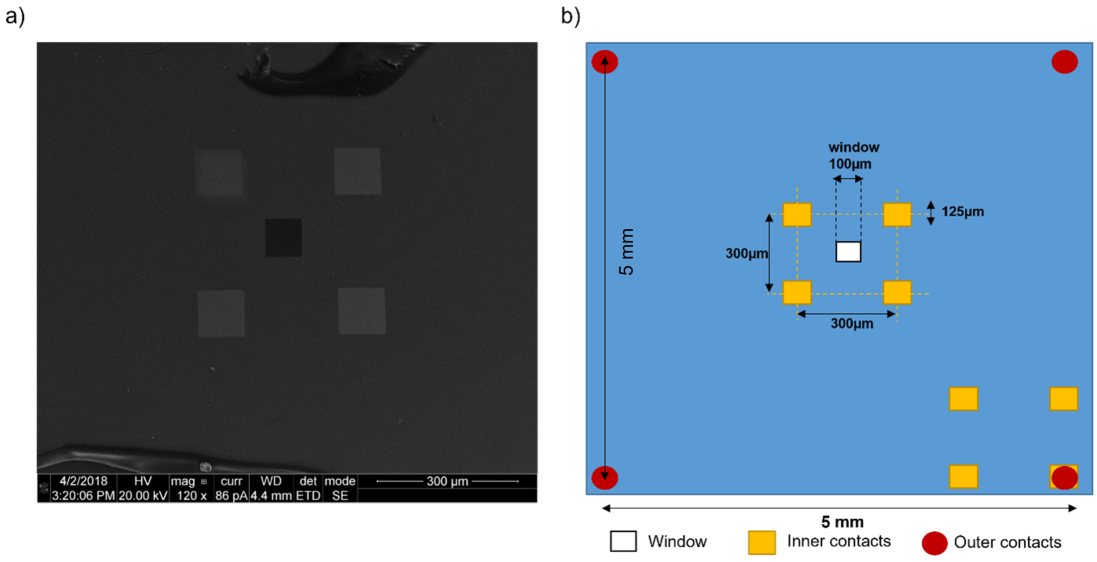

Figure 3.4 Contacts for the MT measurements a) SEM image of the area around the transmission window showing four Pt square pads; b) Diagram of the various wirebond connections and the spacing between all of them.

Chapter 4

Results

4.1 High T magneto-transport (EHE and MR) data

We have carried MT measurements at home to better understand the data we were getting at the APS. The placement of the wire bonds was the same as the ones at the APS, i.e., closely located around the central transmission window. Over time some of these wire bonds broke or burned out, but we have tried our best to place them as close to the original spot as possible. Also, we have created a set of new wire bonds in two additional locations, so, in total, we have three sets of wire bonds. The first set is located at 300 microns around the transmission window, the second set is located at each corner of the sample around 5 mm apart, and the third set is like the first one at 300 microns apart, but located off window, as shown in diagram Figure 3.4.

Fig. 4.1 shows a selection of the data collected on the outer and inner contacts around the window, as well as the off-window contact measurements at room temperature. The EHE and MR signals on the outer contacts in Fig. 4.1 (a) and (b), respectively, show the expected shape for a ferromagnetic film. The EHE data in Fig. 4.1(a) has the shape of the hysteresis curve characteristic of our [Co/Pd] IrMn film and already measured via VSM in Fig. 2.2. Consistent with the VSM data,

the saturation points on the EHE loop on both ends are located at 3500 Oe for all the magnetization loops. The coercive points is 285 Oe for the ascending branch, and -285 Oe for the descending branch. The MR data in Fig. 4.1(b) shows two lobes or arches, typical of MR data on ferromagnetic films. Each arch extents from the nucleation point to the saturation point and peaks at around the coercive point. In our MR data, the two arches (on the ascending and descending branches) are symmetric and reaches about the same height, with a maximum located at $\pm$2000 Oe.

The EHE and MR data collected on the inner contacts shown in Fig. 4.1(c) and (d) respectively is distorted compared to the typical data as measured on the outer contact. We can interpret these distorted shapes as being a combination of the standard EHE and MR signals. The upper right-hand side of the EHE signal when combined with the MR signal would shift up the right-hand lobe as well was decreasing its size. The lower left-hand side of the EHE signal would make the left-hand lobe on the MR data decrease in size, but not as much as the right-hand lobe. Both EHE signals measured on the inner contacts at the APS and at BYU show a signal that is asymmetric. The EHE signal measured on the inner contacts around the transmission window looks very similar to the data collected at the APS, which confirms that it was not an artifact but real signal. The EHE signal measured off-window shown in Fig. 4.1(e) shows a distorted shape, similar to the one measured in Fig. 4.1 (b), except it is flipped. Saturation is reached around -3500 Oe, and 4000 Oe (the discrepancy between the negative and positive saturation points is mostly due to experimental noise). Overall, the off-window signal is consistent with what is measured on-window.

In the next section, we will show that the asymmetric EHE signal on the inner contacts can be modeled as a linear combination of the outer contacts EHE and MR signals. The closeness of the contacts has created a mixed effect where the resulting data may be modeled as a mixture of both EHE and MR signal.

4.2 Effect of microstructration

The magnetization loops we have measured at the APS, have very noticeable asymmetries. As previously explained, we investigated this asymmetry and found that due to the closeness of the wire bonds and the non-equidistance between the wire bonds. We have found that the asymmetric shape can be explain by a mixture of a Hall Effect signal and a MR signal. We have found that a linear combination of both the EHE signal and MR signal can be used to account for these discrepancies. The general form of the model used is $(\mathrm{a} * \mathrm{EHE} + \mathrm{b} * \mathrm{MR})$ where a and b are two scalars to be fitted.

What we have seen from the previous sections is that there is a difference between measurements done on the edges of the sample and measurements done around the transmission window. The data is very much dependent on the placement of the contacts in two distinct ways. First the overall distance the contacts are apart, and second how equally spaced the contacts are from each other. If measurements are taken with the contacts ~5 mm apart the resulting data is different when they are 300 μm apart. With contacts close around the window, there is a "mixing" of the HR signal and the MR signal. which results in a distorted signal. In Fig. 4.3 we see that when the contacts are not placed around the transmission window we still get the same distorted signal again. The setup of the contacts on Fig. 4.3 are with the contacts ~300 μm apart. We also took measurements to see if there was a difference between the on-window and off-window windows. The spacing between off-window contacts were made to be roughly the same as the spacing between contacts on the inner contacts. The fit on the off-window measurement for the most part looks very similar, but the fit parameters a, b are different than in the on-window case. The fitted parmeters for the off-window shown in Fig. 4.2 are a = -0.8 and b = 0.88, so the parameters are about equally weighted. On the fits for the on-window shown in Fig. 4.3 there is more weight towards the b parameter (b = 1.5 with a being close to 1) which is related to the MR component. We evaluated that about $1/3$ of the distortion is due to the window and $2/3$ due to the closeness of the contacts [14].

4.3 Effect of field angle

The experiment at the APS utilized an octupolar magnet for applying a field perpendicular to the surface of the sample. This octupolar magnet allows one to apply a field in any direct we choose. It turned out that during our experiment the applied field was not quite perpendicular to the surface of the sample because of some issues with some of the electromagnet's poles. Because of this we weren't sure how exactly this would effect the resulting data. So, we did more measurements home, at room temperature to see what kind of effect a tilt angle could have on the magnetization loops. Our collected data suggests no effect of the angle of the field/ field tilt on the shape of the magnetization loop. Fig. 4.1 is a summary of collected data at different angles.

The fits shown in fig. 4.2 show the resulting fits at different tilt angles. The tilt angle is the angle formed between the applied field and the surface of the sample. In more recent experiments we have been taking measurements at different angles to study how sensitive the magnetization loop is to a change in the angle. As shown in fig. 4.2 there is not much of a difference between the coefficient values at different angles.

4.4 Low T magneto-transport data using PPMS

Fig. 4.4 show measurements that were done on the Physical Properties Measurement System (PPMS) using a superconducting magnet. At low temperature, after field cooling under a saturating field, the EHE loops show exchange bias as expected. The measured exchange bias for the EHE magnetization loops is 400 Oe. The low temperature MR magnetization loops also exhibit exchange bias. The measured exchange bias for the MR magnetization loop is 300 Oe. From this we should be able to make a prediction of what the exchange bias should be on the APS data. Knowing the amount of exchange bias on the EHE/MR curve will be useful to see if there is a partial loss or complete loss of exchange bias while under x-ray illumination.

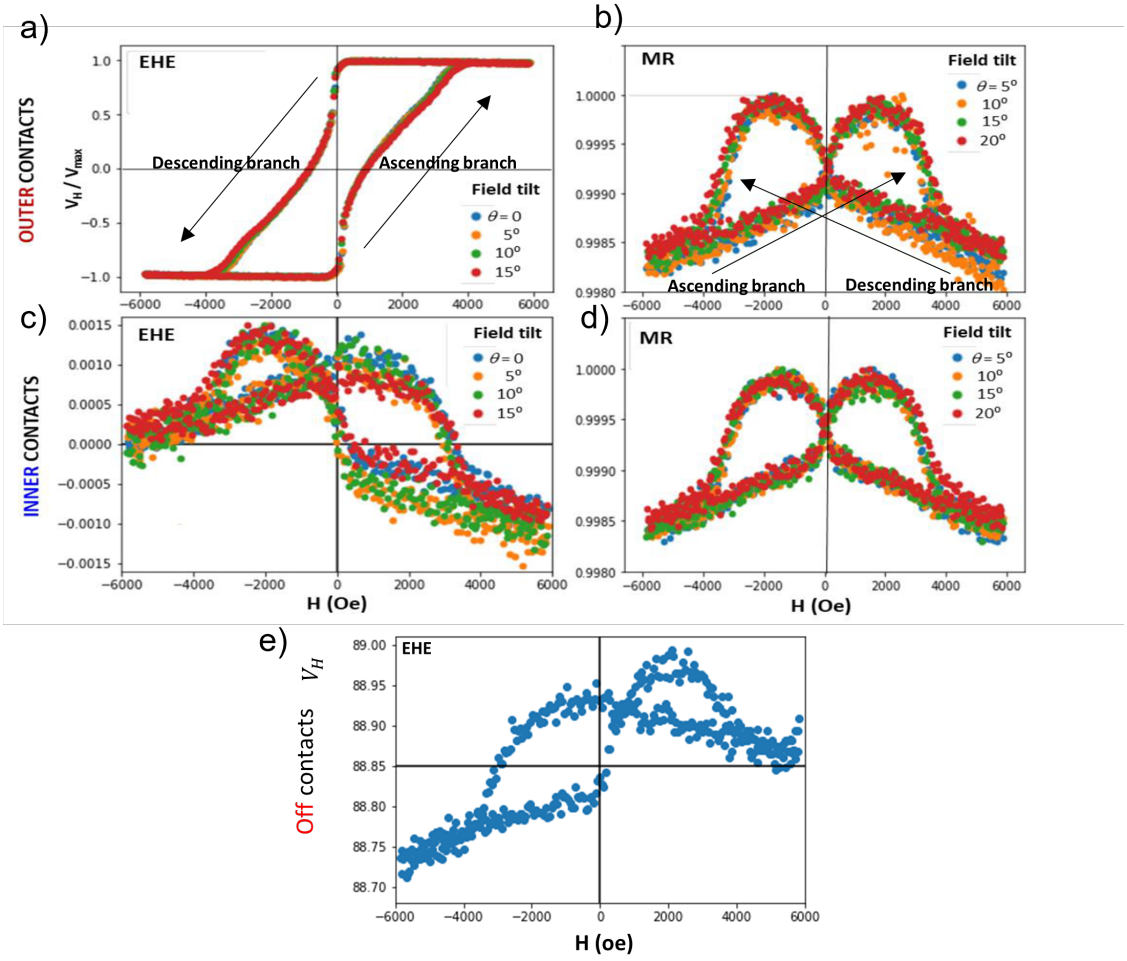

Figure 4.1 EHE and MT data collected at 300 K in the different contact configurations. (a) EHE and (b) MR signals on the outer contacts, (c) EHE and (d) MR signals on the inner on-window contacts, (e) EHE signal on the inner off-window contacts.

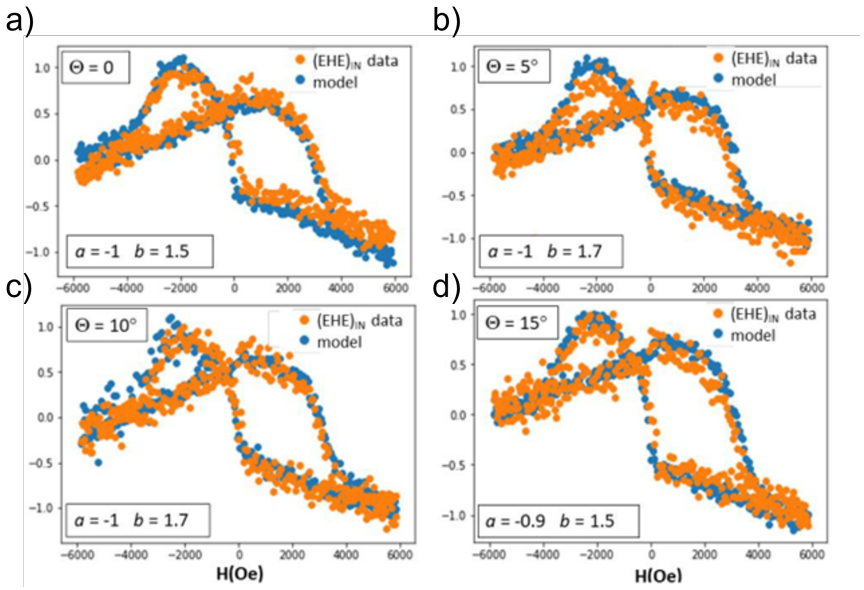

Figure 4.2 EHE data on window contacts collected at 300 K at different field tilt angles: (a) zero degrees, (b) 5°, (c) 10°, and (d) 15° respectively

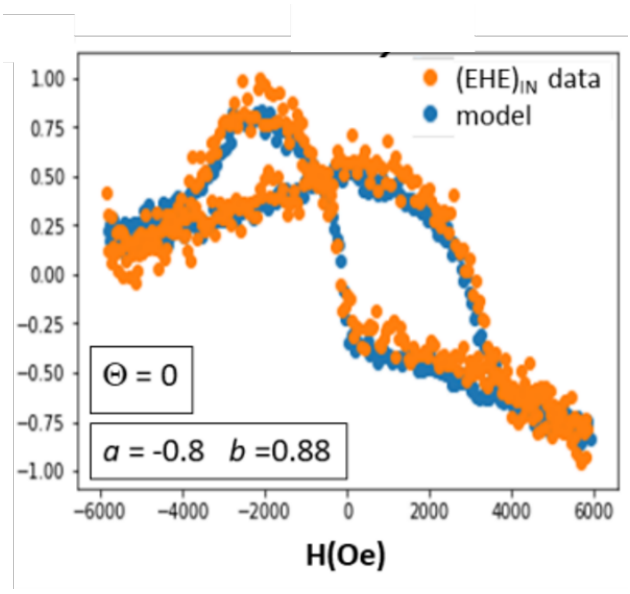

Figure 4.3 EHE data collected at 300 K off-window inner contacts with associated fit

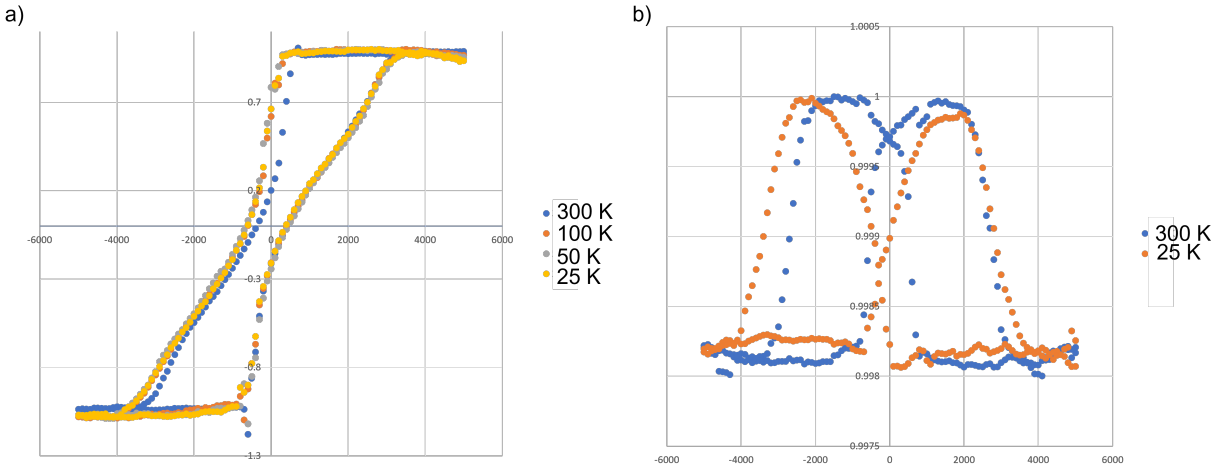

Figure 4.4 MT data meassured with the PPMS cryomagnet and resistivity puck. (a) EHE data measured at 25 K, 50 K, 100 K, and 300 K after field cooling under 5000 Oe. (b) MR data measured at 300 K and at 25 K after field cooling under 5000 Oe.

4.5 Synchrotron EHE data

Finally, we now review the MT data collected in-situ in the synchrotron scattering chamber, while the sample is being illuminated with coherent x-rays and test our hypothesis. The contact setup used for these APS measurements were the inner contact set around the transmission window. Fig. 4.5 shows data collected at 300 K and at 25 K after field cooling under a field of ~5000 Oe. A bias of ~300 Oe was observed at the beginning of the synchrotron experiment, before we start illuminating.

4.6 Effect of x-ray illumination

Fig. 4.6 shows more in-situ MT data, collected under x-ray illumination. One study compares the MT signal collected before, during and after x-ray illumination There is a noticeable effect on the shape of the magnetization EHE loop, in particular the location of the nucleation edge on the descending branch. The longer the sample is illuminated by x-ray, the more the location of the nucleation edge shifts to the right. There is a ~150 Oe loss in the bias during the measured

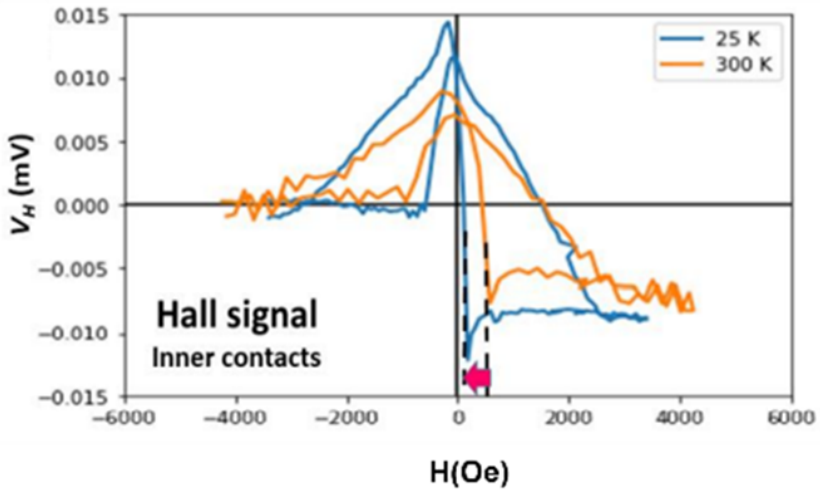

Figure 4.5 Magnetization loops measured at the APS via MT (EHE signal) on our [Co/Pd]/IrMn sample at 300 K and at 25 K after field cooling under a field of 4500 Oe. The arrow indicates the observed field bias of about 300 Oe.

illumination time. This shifting effect reflects an effective loss of field bias, which suggests a progressive destruction of exchange couplings. Despite the loop distortion, the progressive change in the loop and progressive shifting confirms that x-ray illumination can cause a loss of exchange coupling and consequently a loss of MDM in the material.

Although there is, to our knowledge, no existing theory to explain the observed loss of bias, we propose here a brief interpretation for our results. During the illumination of the material by polarized resonant x-rays, the orbital angular momentum carried by the photons interacts with the spin of the electrons in the (2p) band which are excited to the (3d) band. This excitation likely disturbs the local exchange couplings at the interface between the spin in the ferromagnetic Co/Pd layer and the spins in the antiferromagnetic IrMn layer. As a result, the exchange bias is partially lost as we cycle the magnetic field, and so is the MDM.

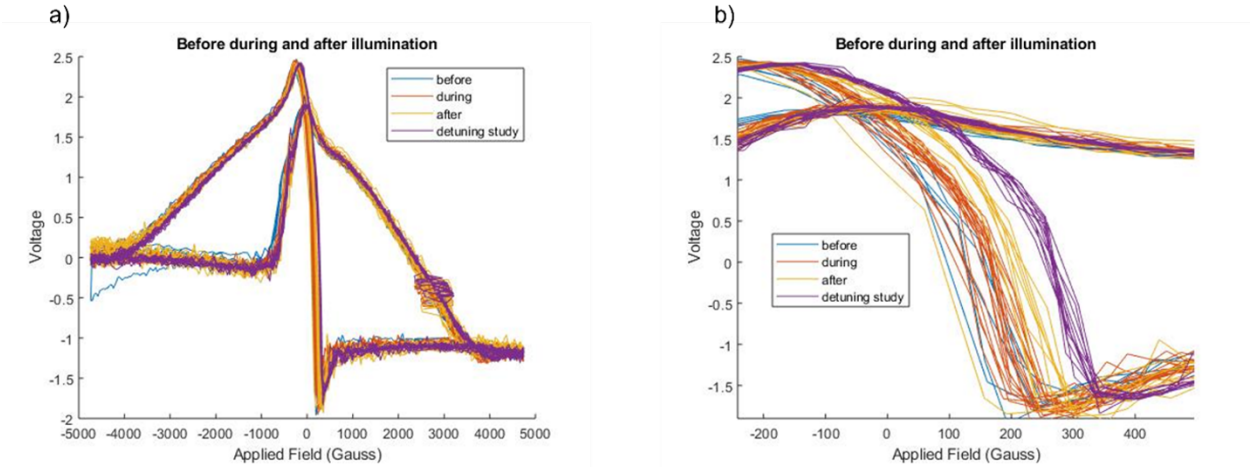

Figure 4.6 MT data measured in the synchrotron scattering chamber during x-ray illumination. a) EHE loop measured at 25 K after field cooling under $H = 5000$ at different stages of the x-ray illumination. b) A zoomed in view of the data in a) around the nucleation point on the descending branch, which shows a progressive loss of bias.

Chapter 5

Conclusion

In this study, we have investigated the possible effect of x-ray illumination on exchange couplings in [Co/Pd]/IrMn layers via magneto-transport. We have observed that the EHE data measured on inner contacts around the transmission window is asymmetric.We observed these asymmetries both in our in-situ synchrotron measurement as well as ex-situ measurements at BYU. These measurements were done at room temperature and below the blocking temperature. These measurements were taken with the EHE and PPMS cryomagnet with the resistivity option. These BYU measurements support the data we observed at the synchrotron, in showing an asymmetric magnetization loop.

We found that the asymmetric EHE data can be expressed as a combination of the regular EHE and MR signals collected on macroscopic contacts. The placement of the wirebonds has a direct effect on the symmetry of the magnetization loop and related to that how much of each signal contributes to the resulting measurement. The resulting signal measured via magneto-transport is a combination of the EHE and MR signals measured on macroscopic contacts. More importantly, we have found that x-ray illumination does have a effect observed exchange bias. The more time the material is exposed to x-rays, the less visible bias is observed which indicates a progressive loss of exchange couplings between the FM and AFM layers. We attribute the bias loss to the interaction between the orbital angular momentum carried by the polarized resonant x-ray photons and the

spins in the material, which then disturbs the exchange couplings between the ferromagnetic and antiferromagnetic layer.

Next directions to investigate include the effect of the illumination duration to see if it would eventually lead to a complete loss of the exchange bias. It would also be interesting to study the reversibility of this process, and see how the lost exchange couplings and lost MDM can possibly be retrieved, via field heating and cooling.

Appendix A

Publication resulting from this work

AIP Advances

Micro-structuration effects on local magneto-transport in [Co/Pd]IrMn thin films

Cite as: AIP Advances **12**, 035327 (2022); https://doi.org/10.1063/9.0000350
Submitted: 01 November 2021 • Accepted: 10 January 2022 • Published Online: 14 March 2022

C. Walker, M. Parkes, C. Olsson, et al.

AIP Advances ARTICLE scitation.org/journal/adv

Micro-structuration effects on local magneto-transport in [Co/Pd]IrMn thin films

Cite as: AIP Advances 12, 035327 (2022); doi: 10.1063/9.0000350
Presented: 27 December 2021 • Submitted: 1 November 2021 •
Accepted: 10 January 2022 • Published Online: 14 March 2022

C. Walker,[1] M. Parkes,[1] C. Olsson,[1] D. Keavney,[2] E. E. Fullerton,[3] and K. Chesnel[1,a)]

AFFILIATIONS

[1] Department of Physics and Astronomy, BYU, Provo, Utah 84602, USA
[2] Advanced Photon Source, Argonne National Laboratory, Lemont, Illinois 60439, USA
[3] Center for Memory and Recording Research, U.C. San Diego, La Jolla, California 92093-0401, USA

Note: This paper was presented at the 15th Joint MMM-Intermag Conference.
[a)] **Author to whom correspondence should be addressed:** kchesnel@byu.edu

ABSTRACT

We measured the local magneto-transport (MT) signal with an out-of-plane magnetic field, including magneto-resistance (MR) and Extraordinary Hall effect (EHE), in exchange-biased [Co/Pd]IrMn thin multilayers that are micro-structured with a 100 μm window. We found that when measured locally around the window, the MT signal deviate from the expected behavior. We studied possible causes, including film micro-structuration, electrical contact geometry as well as magnetic field angular tilt. We found that tilting the magnetic field direction with respect to the normal direction does not significantly affect the MT signal, whereas the positioning and geometry of the contacts seem to highly affect the MT signal. For comparison purposes, we carried these MT measurements using the Van-der-Pauw method on a set of four microscopic contacts directly surrounding the window, and on another set of micro-contacts located outside the window, as well as a set of four contacts positioned several millimeters away of each other at the corners of the wafer. If the contacts are sufficiently far apart, the EHE and MR signals have the expected shape and are not significantly affected by the presence of the window. If, on the other hand, the contacts are micro-positioned, the shape of the EHE signal is drastically deformed, and may be modeled as a mix of the standard EHE and MR signals measured on the outer contacts. Furthermore, if the micro-contacts are located directly around the window, the deformation is amplified, and the weight of the MR signal in the mix is further increased by about 40 %. This suggests that the electron path in the Hall geometry is disturbed by both the proximity of the electrodes and by the presence of the window, which both contribute to the deformation for about two-third and one third, respectively.

INTRODUCTION

Multilayered [Co/Pd]IrMn thin films, as sketched in Fig.1a, exhibit interesting magnetic properties.[1–3] One of these properties is exchange-bias (EB),[4] caused by interfacial couplings between the ferromagnetic (FM) Co/Pd multilayers and the antiferromagnetic (AF) IrMn layers, occurring when the film is field-cooled below its blocking temperature T_B.[5] We found in previous studies[6–8] carried on [[Co (4Å)/Pd (7Å)]$_{x12}$/IrMn(24Å)]$_{x4}$ for which $T_B \sim 275$ K, that these exchange couplings induce remarkable Magnetic Domain Memory (MDM). The observed MDM is the highest and the most extended throughout the magnetization loop when the cooling field is close to zero (remanence).[9] At remanence, the magnetic domains in the F layer tend to form a maze pattern, like the one illustrated in Fig. 1b, which gets imprinted in the AF layer upon cooling. We carried these studies using synchrotron x-ray radiation, which allows probing the domain pattern morphological changes at the nanoscale while applying a magnetic field in-situ.[10] However, recently, we observed an unexpected loss of MDM upon field cycling. We have been investigating possible reasons for the MDM loss, including x-ray illumination effects. For these investigations, we used in-situ magneto-transport (MT) while under x-ray illumination, to see if the MDM loss may be accompanied by a loss of EB. In practice, EB consists in the biasing of the magnetization loop with the respect to the applied magnetic field, in the direction opposite to the direction of the previously applied cooling field. Our earlier magnetization

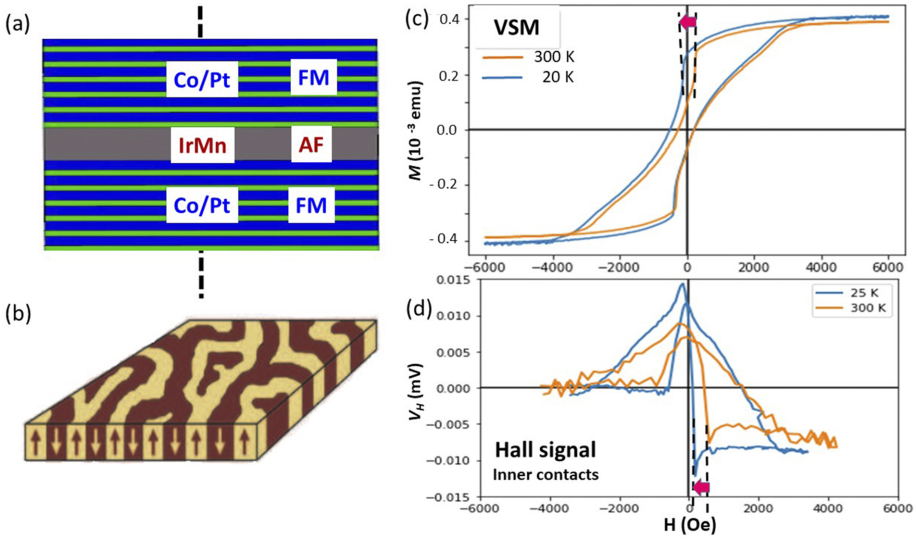

FIG. 1. (a) Sketch of the $[[Co\ (4Å)/Pd\ (7Å)]_{x12}/IrMn(24Å)]_{x4}$ multilayer structure; (b) Illustration of magnetic domain pattern forming in the film near remanence; (c) Magnetization loops measured via VSM at 300 K and at 20 K after field cooling under a + 6000 Oe field; (d) Magnetization loops measured via EHE under a current of 100 mA on inner contacts at 300 K and 25 K after field cooling under +4750 Oe. In both VSM and EHE measurements, the cooling field was well above saturation point $H_s \sim 3200$ Oe.

measurements on $[[Co\ (4Å)/Pd\ (7Å)]_{x12}/IrMn(24Å)]_{x4}$, shown in Fig.1c using Vibrating Sample Magnetometry (VSM), indicate a bias field as high as 200 Oe at 20 K. When measuring EB via MT, we could observe a biasing effect consistent with the VSM measurements. However, we found that the shape of the Extraordinary Hall Effect (EHE) signal (see Fig.1d) is deformed with respect to the expected magnetization loop shape. This paper investigates possible reasons for this deformation.

METHODOLOGY

The synchrotron x-ray magnetic scattering measurements were carried at the Advanced Photon Source, beamline 4-ID-C, in a vacuum chamber equipped with an in-situ octupole magnet. To allow x-ray scattering measurements in transmission geometry, the $[[Co\ (4Å)/Pd\ (7Å)]_{x12}/IrMn(24Å)]_{x4}$ thin films were deposited onto 100 nm thick Si_3N_4 membranes supported by silicon wafers that have a 100 μm window at their center. To enable MT measurements, the films were electrically hooked to a circuit board with ultra-thin 20 μm wires soldiered via wire-bonding, as seen in Fig.2a. The electrical contacts were grouped by sets of four, to enable both Extraordinary Hall Effect (EHE) and magneto-resistance (MR) measurements using the Van-der-Pauw method[11,12] with a magnetic field applied out-of-plane.

To study the effect of x-ray illumination on the exchange couplings and a possible loss of EB, the MT signal was measured locally, as close as possible to the illuminated window. For this purpose, we created four electrical contacts nearby the central window by depositing four Pt pads using Focused Ion Beam (FIB). The geometry and location of these four pads are shown in the sketch Fig.2b and in the Scanning Electron Microscopy (SEM) image Fig.2c. Each pad has a shape of a 125 x 125 μm^2 square, that is 100 nm thick. The four pads are diagonally located by the four corners of the window at a distance of 300 μm of each other. Along the diagonal, the distance between pads is about 425 μm center-to-center and the central window covers about 33% of that distance. Additional to these micrometric "inner" contacts located around the window (ON-window), we created, for comparison purposes, another set of four "inner" contacts with similar geometry but located outside the window (OFF-window), as well as a set of four "outer" contacts located by the four corners of the wafer at about 5 mm of each other, as schematically represented in Fig.2b.

When measuring the MT signal on the inner contacts while using the octupole magnetic chamber, we found that the EHE signal, shown in Fig.1d, was deformed with respect to the expected hysteresis loop, as measured via VSM (see Fig.1c). The EHE signal appeared like a folded hysteresis loop.

To investigate the origin of this deformation, we conducted a series of MT measurements in our laboratory at BYU. One investigation consisted in comparing the MT signal on the inner contacts to the MT signal on the outer contacts, used as a reference. Another investigation consisted in comparing the MT signal measured on the

AIP Advances ARTICLE scitation.org/journal/adv

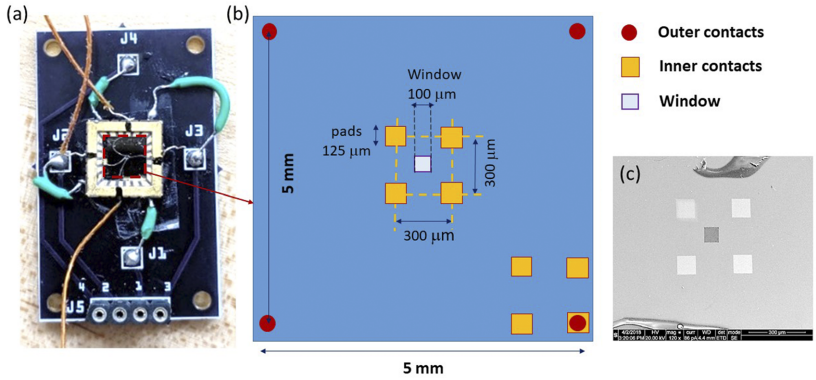

FIG. 2. (a) Picture of the electrical board on which the film is mounted and electrically connected via wire-bonding; (b) Sketch showing the location of the outer contacts at the four corners of the film and the location of the inner contacts surrounding the central 100 μm window; (c) SEM image of the padded inner contact deposited via FIB surrounding the 100 μm window.

inner contacts ON-window and OFF-window to identify possible effects caused by the window itself. Additionally, we studied possible effects caused by tilting the applied magnetic field with respect to the direction normal to the film surface. Indeed, during the synchrotron measurement, one of the eight poles of the octupole electromagnet failed, causing a tilting of the applied magnetic field with respect to the direction of the x-rays. In addition, due to space constraints, the sample holder was also tilted, causing a tilt of the film with respect

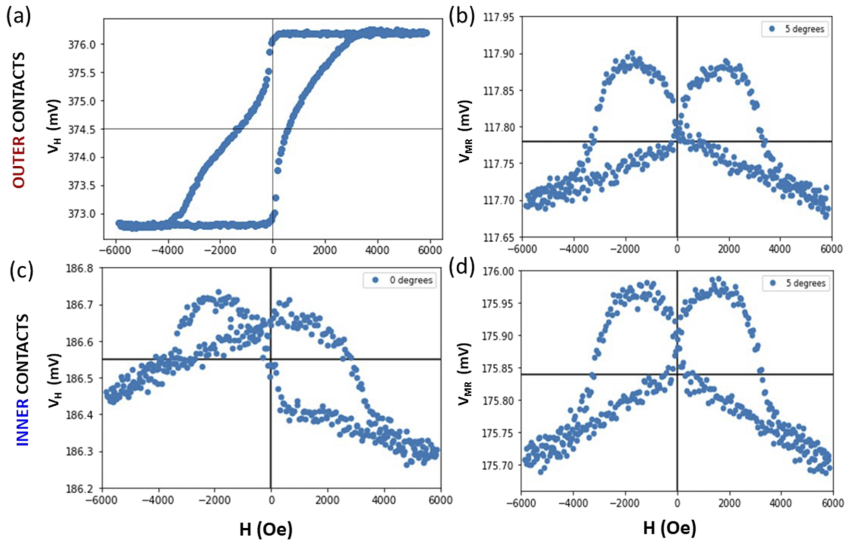

FIG. 3. (a,b) Actual MT signal measured on the ***outer contacts:*** (a) EHE signal and (b) MR signal; (c,d) Actual MT signal measured on the ON-window ***inner contacts***: (c) EHE signal and (d) MR signal. All the measurements were carried under a current of 100 mA.

AIP Advances ARTICLE scitation.org/journal/adv

to the x-ray direction. The combination of these two angular deviations resulted in a total tilt between the magnetic field direction and normal to the film surface up to about 25°.

The BYU MT measurements were carried in a bipolar electromagnet. The EHE signal, on one hand, was obtained by measuring the voltage in the transverse direction with respect to the applied current, while the magnetic field is applied perpendicular to the film. For the EHE data, averages between such transverse measurements measured at 90° of each other were taken. The MR signal, on the other hand, was obtained by measuring the voltage in the direction parallel to the applied current using the four contacts and applying the Van-der-Pauw method, where four different configurations were averaged to eliminate possible structural asymmetries.[12]

RESULTS AND DISCUSSION

The MT signal measured on the outer contacts, displayed in Fig.3 a,b, shows a behavior typical of ferromagnetic materials. The averaged EHE signal in Fig.3a has the shape of a hysteresis loop, consistent with the VSM signal. The averaged MR signal in Fig.3b has a symmetrical double-lobe shape typical of magneto-resistance in ferromagnetic thin films with perpendicular magnetic anisotropy.[13,14] The measured MR voltage is around 118 mV for a current of 100 mA, corresponding to a resistance of $R_{//} \approx 1.2\Omega$ with magneto-resistance variation $\Delta R \approx 210^{-3}\Omega$.

The MT signal measured on the ON-window inner contacts however behaves differently compared to the MT signal measured on the outer contacts. The measured EHE signal in Fig.3c has a deformed shape with respect to the expected hysteresis loop. The deformed shape looks like a hysteresis loop folded onto itself in an asymmetrical way, leading to two apparent hysteresis loops, a smaller one and a bigger one. On the other hand, the average MR signal in Fig.3d is similar to the MR signal measured on the outer contacts (Fig.3b), still showing a symmetrical double-lobe shape. The measured MR voltage is around 178 mV for a current of 100 mA, corresponding to a resistance $R_{//} \approx 1.8\Omega$, with magneto-resistance variation $\Delta R \approx 310^{-3}\Omega$.

The dependence with magnetic field tilt was studied by tilting the sample holder with respect to the electromagnet axis. The setup allowed a tilt up to 20°. Data collected at various angles is plotted in Fig.4 For comparison purposes, the data in Fig.4 was normalized to the maximum value (plotting $V/V_{\max}$) after recentering the signal, so that both the EHE and MR magnetization loop signal varies between − 1 and +1. The data shows no significant effect of magnetic field tilt on the shape of the EHE and MR signals, neither on the outer contacts nor on the inner contacts. This observation rules out any correlation between the observed EHE signal deformation and the actual magnetic field tilt during the synchrotron measurement.

It then appears that the deformation of the EHE signal observed on the inner contacts is principally due to micro-structuration

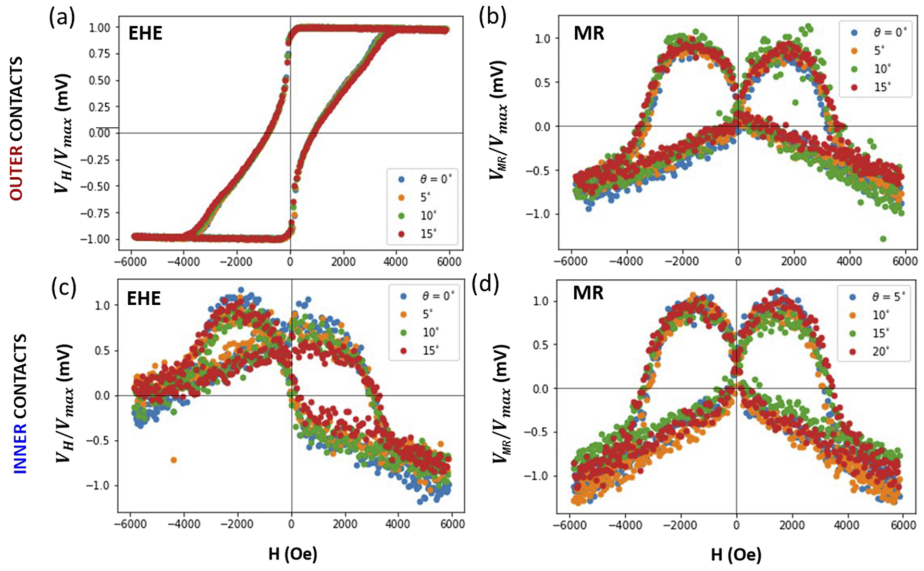

FIG. 4. (a,b) Normalized MT signal measured on the ***outer contacts:*** (a) EHE signal and (b) MR signal; (c,d) Normalized MT signal measured on the ON-window ***inner contacts***: (c) EHE signal and (d) MR signal. Measurements at various angles from 0 to 20° are displayed.

AIP Advances ARTICLE scitation.org/journal/adv

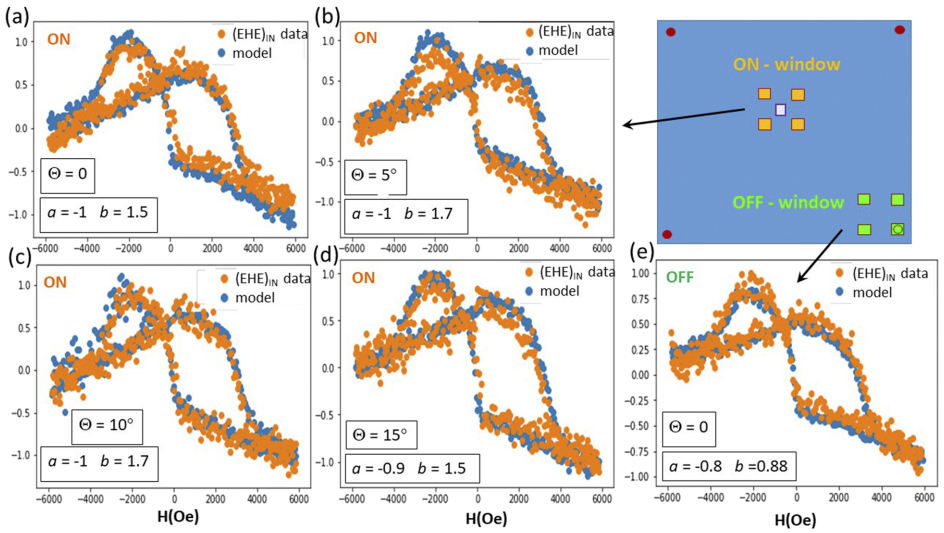

FIG. 5. Modeling of the EHE signal measured on two sets of inner contacts: (a-d) around the window (ON-window) and (e) outside the window (OFF-window) for comparison. The location of the sets of contacts is schematically represented on the diagram. The data was collected as follows: ON–window at an angle of (a) $\theta = 0$; (b) $\theta = 5^{\circ}$; (c) $\theta = 10^{\circ}$; (d) $\theta = 15^{\circ}$; (e) OFF–window at an angle of $\theta = 0$. For each data set, the model uses a linear combination of the normalized EHE and MR signals measured on the outer contacts, as follows: $(EHE)_{IN} = a * (EHE)_{OUT} + b * (MR)_{OUT}$.

(window) effects and geometry of the contacts. When measuring the MT signal using the inner contacts, the electron path is significantly disturbed by the presence of the window, which occupies 33% of the distance between electrodes, and also by the relative width of the pads (125 μm) with respect to the inter-pad distance (300 μm), that occupies about 45 % of that inter-electrode distance. This suggests that electrons may not travel on straight paths between diagonally opposite contacts, but instead may deviate from the straight path to get around the central window. In this process, some electrons may end up hitting adjacent contacts instead of opposite contacts, causing some mixing between EHE and MR signals.

To support this hypothesis, we attempted modeling the EHE signal measured on inner contacts by using a linear combination of the EHE and MR signals measured on the outer contacts as follows:

$$(EHE)_{IN} = a * (EHE)_{OUT} + b * (MR)_{OUT}$$

The modeling results displayed in Fig. 5 show that one can indeed reconstruct the asymmetric shape of $(EHE)_{IN}$ by mixing the $(EHE)_{OUT}$ and $(MR)_{OUT}$ signals with coefficients a and b in opposite signs. The ratio $|b/a|$ for the EHE signal for the ON-window inner contacts ranges between 1.5 and 1.7 for the various sets measured at different tilt angles.

To further disentangle possible separate effects caused by the window on one hand and by the contact geometry on the other hand, we measured the EHE signal on a set of inner contacts located OFF-window, as illustrated in Fig.5. The measured OFF-window EHE signal, shown in Fig.5e, has a shape similar to the ON-window EHE signal. The modeling of the OFF-window EHE signal leads to a ratio $|b/a| \approx 1.1$. The significant change in the $|b/a|$ ratio from about 1.1 up to 1.6 when moving from the OFF-window to ON-window contacts confirms that the window does contribute significantly to the deformation of the EHE signal. While the proximity of the contacts induces about 2/3 (~70%) of the deformation, the presence of the window induces another 1/3 (~30%) of the deformation. This suggests possible pulling effects at the edge of the window, which could be caused by misalignments between the plane of the film and the plane of the window, as well as morphological defects or discontinuities in the structure of the multilayered film at the edges of the window. These micro-structuration effects are therefore non-negligeable when measuring the MT signal locally and must be taken into consideration.

CONCLUSION

We have probed the local magneto-transport (MT) signal, including magneto-resistance (MR) and Extraordinary Hall Effect (EHE), in exchange-biased $[[Co\ (4Å)/Pd\ (7Å)]_{x12}/IrMn(24Å)]_{x4}$ thin films that are micro-structured with a central 100 μm window. We carried these measurements using the Van-der-Pauw method on

three sets of four contacts: a set of outer contacts located 5 mm apart at the four corners of the film; a set of inner contacts, made of 125 μm pads located at 300 μm of each other, surrounding the central 100 μm window, and another set of inner contacts with same geometry, located outside the window toward the corner of the wafer, for comparison purposes. We found that when measured on the outer contacts, the MT signal has the expected shape, with the EHE signal forming a hysteresis loop consistent with magnetometry measurements, and the MR signal showing a symmetrical double-lobe shape. When measured on the inner contacts, the MR signal still shows the symmetrical double-lobe shape, however the EHE signal is significantly deformed, looking like an asymmetric folded hysteresis loop. This deformation was observed both with the ON-window contacts and the OFF-window contacts. The deformed $(EHE)_{IN}$ shape may be reconstructed by mixing the $(EHE)_{OUT}$ and $(MR)_{OUT}$ signals measured on the outer contacts. The relative MR/EHE weight ratio was found to be in the range of 1.5 to 1.7 for the ON-window contacts, and around 1.1 for the OFF-window contacts. This suggests that when EHE is probed locally with electrodes at close proximity, the electrons are not traveling in a straight path between diagonally opposite contacts but a portion of them hit the adjacent contacts instead, leading to a mix of MR and EHE signals. Furthermore, the presence of the window increases the weight of the MR signal in the deformation (an additional 40%). This suggests that the window causes pulling effect due to morphological misalignments and defects occurring at the edges of the window. Additionally, we found that moderately tilting the magnetic field with respect to the film normal direction is not affecting the shape of the MT signal significantly. The observed deformation of the EHE signal is mainly due to the micro-structuration of the film and the proximity of the inner contacts with the central window covering 33% of the path between contacts.

In order to measure effects of x-ray illumination on exchange-bias, it is however necessary to probe the MT signal locally around the illuminated region of the film, which necessitates some micro-structuration. Our current setup induces a deformation of the EHE signal. A solution to this issue may be to etch the [Co/Pd]IrMn film in the shape of a cross around the central window so to guide the electrons path in the desired direction for the EHE measurement. That being said, it is interesting to note that, despite the observed deformation, the EHE signal measured on the inner contacts with the current setup still shows the biasing effect when the film is cooled from 300 K down to 20 K below the blocking temperature, consistent with magnetometry measurements. So, even when its shape is deformed due to micro-structuration, the EHE signal may be used to measure exchange bias and monitor its dependence with various parameters such as temperature or x-ray illumination.

ACKNOWLEDGMENTS

This work was supported by the Research Experience for Undergraduate Students (REU) funding program, grant #1757998, at the National Science Foundation (NSF) as well as by the Advanced Photon Source at Argonne National Laboratory, a Department of Energy facility.

AUTHOR DECLARATIONS

Conflict of Interest

The authors have no conflicts to disclose.

DATA AVAILABILITY

The data that support the findings of this study are available from the corresponding author upon reasonable request.

REFERENCES

[1]W.-B. Wu, J. Kasiuk, T. N. A. Nguyen, J. Fedotova, J. Przewoznik *et al.*, Phys. Chem. Chem. Phys. **22**, 3661–3674 (2020).
[2]W.-B. Wu, J. Kasiuk, J. Fedotova, T. N. A. Nguyen, T. H. T. Trinh *et al.*, International J. Nanoscience **18**, 1940017 (2019).
[3]W. J. Kong, Y. R. Ji, X. Zhang, H. Wu, Q. T. Zhang *et al.*, Appl. Phys Lett. **109**, 132402 (2016).
[4]W. H. Meiklejohn, Phys. Rev. **102**, 1413 (1956).
[5]S. Maat, K. Takano, S. S. Parkin, and E. E. Fullerton, Phys. Rev. Lett. **87**, 087202 (2001).
[6]K. Chesnel, E. E. Fullerton, M. J. Carey, J. B. Kortright, and S. D. Kevan, Phys. Rev. B **78**, 132409 (2008).
[7]K. Chesnel, J. A. Nelson, S. D. Kevan, M. J. Carey, and E. E. Fullerton, Phys. Rev. B **83**, 054436 (2011).
[8]K. Chesnel, B. Wilcken, M. Rytting, S. D. Kevan, and E. E. Fullerton, New J. Physics **15**, 023016 (2013).
[9]K. Chesnel, A. Safsten, m. Rytting, and E. E. Fullerton, Nat. Comm. **7**, 11648 (2016).
[10]K. Chesnel, J. Nelson, B. Wilcken, and S. D. Kevan, J. Synch. Rad. **19**, 293–306 (2012).
[11]L. J. van der Pauw, "A method of measuring specific resistivity and Hall effect of discs of arbitrary shape," Phillips. Res. Repts. **13**, 1–9 (1958).
[12]A. A. Ramadan, R. D. Gould, and A. Ashour, Thin Solid Films **239**, 272–275 (1994).
[13]W.-B. Wu, J. Kasiuk, T. N. A. Nguyen, J. Przewoźnik, J. Fedotova *et al.*, J. Appl. Phys. **127**, 223904 (2020).
[14]R. Law, R. Sbiaa, T. Liew, and T. C. Chong, Appl. Phys. Lett. **91**, 242504 (2007).

Bibliography

[1] J. Stohr and H. C. Siegmann, *Magnetism: From Fundamentals to Nanoscale Dynamics*

[2] I. K. Schuller, R. Morales, X. Batlle, U. Nowak, and G. Guntherodt, "Role of the antiferromagnetic bulk spins in exchange bias," Journal of Magnetism and Magnetic Materials **416,** 2–9 (2014).

[3] S. Foner, "Versatile and Sensitive Vibrating-Sample Magnetometer," The Review of Scientific Instruments **30,** 548 (1959).

[4] G. van der Laan, "Applications of soft x-ray magnetic dichroism," Journal of Physics: Conference Series 430 (2013).

[5] L. J. V. der Pauw, "A Method of Measureing Specific Resistivity and Hall Effect of Discs of Arbitrary Shape," Semiconductor Devices: Pioneering Papers pp. 174–182 (1991).

[6] G. van der Laan and A. I. Figueroa, "X-ray magnetic circular dichroism– A versatile tool to study magnetism," Coordination Chemistry Reviews **277-278,** 95–129 (2014).

[7] K. Chesnel, A. Safsten, M. Rytting, and E. E. Fullerton, "Shaping nanoscale magnetic domain memory in exchange-coupled ferromagnets by field cooling," Nature Communications **7,** 1–8 (2016).

[8] K. Chesnel, E. E. Fullerton, M. J. Carey, J. B. Kortright, and S. D. Kevan, "Magnetic memory in ferromagnetic thin films via exchange coupling," Physical Review B 78 (2008).

[9] J. Nelson, B. Wilcken, and K. Chesnel, "Persistence of magnetic domain memory through field cycling in exchange biased thin films," J. Utah Acad. Sci **87,** 267–274 (2010).

[10] K. Chesnel, J. Nelson, S. Kevan, M. J. Carey, and E. E. Fullerton, "Oscillating spatial dependence of domain memory in ferromagnetic films mapped via x-ray speckle corrleation," Physical Review B 83 (2011).

[11] K. Chesnel, J. Nelson, B. Wilcken, and S. Kevan, "Mapping spatial and field dependence of magnetic domain memory by soft X-ray speckle metrology," Journal of Synchrotron Radiation **19,** 293–306 (2012).

[12] K. Chesnel, B. Wilcken, M. Rytting, S. Kevan, and E. E. Fullerton, "Mapping spatial and field dependence of magnetic domain memory by soft X-ray speckle metrology," New Journal of Physics 15 (2013).

[13] K. Chesnel, *Nanoscale Magnetic Domain Memory* Book chapter in *"Magnetism and Magnetic Materials" (2018).*

[14] C. Walker, M. Parkes, C. Olsson, D. Keavney, E. E. Fullerton, and K. Chesnel, "Microstructuration effects on local magneto-transport in [Co/Pd]IrMn thin films," AIP Advances 12 (2022).